Cancer Therapy: Preclinical

LY2109761 Attenuates Radiation-Induced Pulmonary Murine Fibrosis via Reversal of TGF-β and BMP-Associated Proinflammatory and Proangiogenic Signals

Paul Flechsig[1,3], Monika Dadrich[1,3], Sebastian Bickelhaupt[1], Jürgen Jenne[1], Kai Hauser[1], Carmen Timke[1], Peter Peschke[1], Eric W. Hahn[1], Hermann-Josef Gröne[2], Jonathan Yingling[4], Michael Lahn[4], Ute Wirkner[1], and Peter E. Huber[1]

Abstract

Purpose: Radiotherapy is used for the treatment of lung cancer, but at the same time induces acute pneumonitis and subsequent pulmonary fibrosis, where TGF-β signaling is considered to play an important role.

Experimental Design: We irradiated thoraces of C57BL/6 mice (single dose, 20 Gy) and administered them a novel small-molecule TGF-β receptor I serine/threonine kinase inhibitor (LY2109761) orally for 4 weeks before, during, or after radiation. Noninvasive lung imaging including volume computed tomography (VCT) and MRI was conducted 6, 16, and 20 weeks after irradiation and was correlated to histologic findings. Expression profiling analysis and protein analysis was conducted in human primary fibroblasts.

Results: Radiation alone induced acute pulmonary inflammation and lung fibrosis after 16 weeks associated with reduced life span. VCT, MRI, and histology showed that LY2109761 markedly reduced inflammation and pulmonary fibrosis resulting in prolonged survival. Mechanistically, we found that LY2109761 reduced p-SMAD2 and p-SMAD1 expression, and transcriptomics revealed that LY2109761 suppressed expression of genes involved in canonical and noncanonical TGF-β signaling and downstream signaling of bone morphogenetic proteins (BMP). LY2109761 also suppressed radiation-induced inflammatory [e.g., interleukin (IL)-6, IL-7R, IL-8] and proangiogenic genes (e.g., ID1) indicating that LY2109761 achieves its antifibrotic effect by suppressing radiation-induced proinflammatory, proangiogenic, and profibrotic signals.

Conclusion: Small-molecule inhibitors of the TGF-β receptor I kinase may offer a promising approach to treat or attenuate radiation-induced lung toxicity or other diseases associated with fibrosis. *Clin Cancer Res; 1–12. ©2012 AACR.*

Introduction

Radiotherapy is a mainstay of lung cancer treatment. Minimizing radiation-induced lung injury (RILI) is an important goal of radiooncological therapy. Radiation-induced tissue responses can be grouped into 3 phases, acute (days), subacute (weeks), and chronic (months to years) tissues responses (1–3). While successful studies have been carried out in rodents to reduce lung injury following radiation or chemotherapy, no effective treatments are available in humans in particular for processes, which eventually lead to radiation-induced lung fibrosis (RILF; refs. 4, 5). RILF is similar to other forms of pulmonary fibrosis, either of iatrogenic origin such as from chemotherapy or surgery or idiopathic (6). Irrespective of the initial cause, fibroblast replication with excessive extracellular matrix deposition is the hallmark of the disease. The clinical manifestation includes progressive dyspnea, deterioration of pulmonary function, and interstitial fluid accumulation resulting in respiratory failure. The motivation to investigate potential treatment options for RILI and RILF is evident and may also have an impact on treatment for idiopathic pulmonary fibrosis (IPF), which is a frequent form of lung fibrosis with a prevalence of 16 to 18 per 100,000 and shares many pathologic similarities with RILF (7, 8).

The cytokine TGF-β is a multifunctional regulator of cell growth and differentiation expressed in response to injuries (9, 10, 11). It is considered to play a key role in radiation-

Authors' Affiliations: [1]Radiation Oncology, [2]Molecular Pathology, German Cancer Research Center and University Hospital Center Heidelberg, and [3]Diagnostic and Interventional Radiology, University Hospital Center Heidelberg, Heidelberg, Germany; and [4]Oncology Early Clinical Investigation, Lilly Research Laboratories, Indianapolis, Indiana

Corresponding Author: Peter E. Huber, Radiation Oncology, German Cancer Research Center (DKFZ)/University of Heidelberg Medical Center, 280 Im Neuenheimer Feld, Heidelberg 69120, Germany. Phone: 49-6221-42-2515; Fax: 49-6221-42-2442; E-mail: p.huber@dkfz.de

Translational Relevance

Radiotherapy is an effective treatment modality for cancer with limitations due to acute and chronic toxicities, where TGF-β plays a key role. Here, we show that LY2109761, a TGF-β receptor I(II) kinase inhibitor, which is effective as anticancer compound in preclinical models, also attenuates radiation-induced pneumonitis and lung fibrosis with increased mouse survival which is dramatically reduced after thoracic radiation. Our signaling data suggest that anti-inflammation and antifibrosis signaling are strikingly similar to the respective effects involved in the anticancer effects of LY2109761 thus linking fibrosis and cancer therapy. With the clinical availability of compounds with similar properties which are currently in phase I/II trials as cancer therapeutics, our study suggests that small-molecule inhibitors of TGF-β signaling may offer a promising approach to treat radiation-associated toxicity in radiotherapy of lung cancer and in other tumor entities, but moreover may imply potentially a simultaneous improvement of anticancer effects.

induced normal tissue damage, in particular in RILI and RILF (1, 2, 6). TGF-β is upregulated in mouse lungs hours to weeks after radiation (12). In wound healing TGF-β enhances interleukin (IL)-1 production in monocytes, which in turn has a mitogenic effect on fibroblasts. Therefore, inhibiting the TGF-β signaling pathway has the potential to reduce RILI and RILF (13, 14).

Activated TGF-β dimers interact with specific cell membrane receptors, consisting of 2 homodimers of TGF-β receptor I (RI) and TGF-β receptor II proteins (RII). Once the ligand/receptor complex is formed, intracellular effector molecules are phosphorylated by the receptor to induce numerous intracellular pathways, among these the canonical Smad2/Smad3-dependent pathway (15).

Here, we used the orally available novel TGF-β receptor I kinase inhibitor LY2109761 (13) in a murine model of RILI and fibrosis. Pulmonary toxicity was elicited by a 20-Gy single dose radiation to the thorax. Mice were observed for more than 6 months, the time necessary to develop pulmonary fibrosis (16–18). Noninvasive radiological methods (MRI and volume computed tomography, VCT; ref. 19), clinical and survival estimations, as well as histology showed morphologically and quantitatively the beneficial effects of LY2109761 on RILI and RILF. Signaling and pathway analyses showed how LY2109761-normalized radiation induced TGF-β, bone morphogenetic protein (BMP), proinflammatory and proangiogenic signaling which together resulted in an attenuation of the lung fibrosis phenotype.

Materials and Methods

Experimental protocol, animal treatment, and reagents

Female C57BL/6 mice (Charles-River-Viga) were irradiated with a single dose of 20 Gy photon radiation (RT; Siemens) limited to the chest. LY2109761 was administered by oral gavage twice daily for 4 weeks at a dose of 50 mg/kg body weight dissolved in 1% carboxymethylcellulose sodium (CMS) USP. Mice were randomly distributed to 6 groups (30 animals for each group, total 180 animals; Fig. 1): group 1 (LY, RT), LY2109761 treatment started 4 weeks before RT; group 2 (LY, RT, LY), LY2109761 treatment started 2 weeks before RT and continued for 2 weeks after RT; group 3 (RT, LY), LY210976 started 1 day after RT; group 4 (LY), LY2109761 was given over 4 weeks without RT; group 5 (RT), only RT; group 6 (control), only CMS. The metabolically stable TGF-β-RI inhibitor LY2109761 was kindly provided by Eli Lilly and Company with additional weak inhibitory effects for TGF-β-RII (13). At week 20 the projected and planned endpoint for the study was reached and the last imaging studies (VCT, MRI) were conducted. The animals were followed for another 5 to 6 weeks (~6 months) to assess clinical outcome and survival.
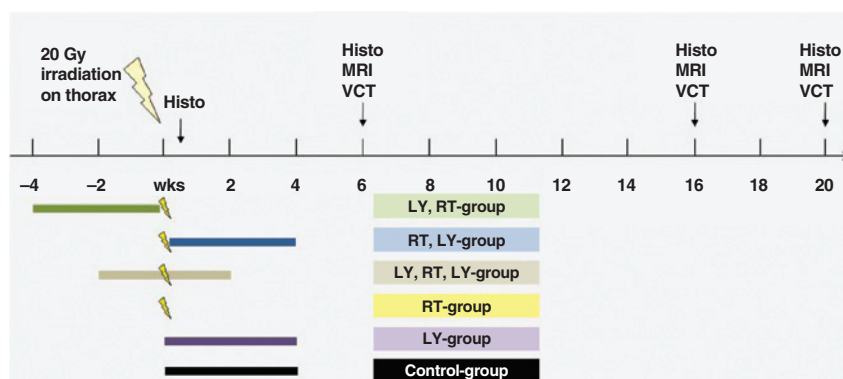
Figure 1. Treatment schedule. Design of the radiation and treatment arms. Mice were irradiated with a single dose of 20 Gy to the thorax at time point zero to initiate pulmonary fibrosis and were treated with the small-molecule TGF-β-RI kinase inhibitor LY2109761 for 4 weeks before (green; LY, RT-group), during (brown; LY, RT, LY-group); or after the irradiation (blue; RT, LY-group). Only irradiated mice (yellow; RT-group), LY without irradiation (purple; LY-group), and sham-treated mice (black) served as controls. Mice were monitored by histology and by noninvasive radiological methods allowing for longitudinal analyses.

VCT in mouse lungs

VCT provides high resolution mice lung imaging (16, 18). We randomly selected 3 mice from each group at weeks 6, 16, and 20 for VCT examination using a Siemens Flat-Panel-Volume-CT-Scanner (80 kV, 50 mAS).

Lung density was expressed as VCT intensity units in analogy to Hounsfield units used in clinical CT scanners. Slices of lung images were made at the tracheal bifurcation and the maximum cardiac diameter. In each selected slice 4 regions of interest (ROI) were defined: left and right anterior, left and right posterior. A total of 8 density values per lung were determined and the arithmetic mean $\pm$ SD defined the representative VCT intensity as a quantitative parameter for lung fibrosis. The same 3 mice were also used for MRI and histology. Some additional animals were used for histology at intervals when no imaging was scheduled.

MRI in mouse lungs

We used MRI for mice lungs (Siemens Magnetom Symphony Syngo MR 2004A, 1.5 Tesla). One advantage of MRI is that the signal characteristics in T2-weighted images have the potential to differentiate between pulmonary fibrosis and pulmonary edema. Three mice were randomly selected from each group for chest MRIs at weeks 6, 16, and 20 after radiation.

Lung histology and immunohistochemistry

Three mice per group were euthanized at day 2, weeks 6, 16, and 20 after radiation. Lungs were fixed by instillation of 4% formalin in PBS into the tracheae, embedded in paraffin, sectioned at 5 μm, and stained with haematoxylin–eosin (H&E), Goldner–Elastika and Sirius Red. Inflammatory cells were counted in 10 randomly chosen slides from each of the 3 animals and septal thickness was determined. p-SMAD2 (Cell Signaling, #3108) was detected according the manufacturer's instructions and 3,3'-diaminobenzidine as chromagen and scored semiquantitatively [rank scale (0, 1, 2, 3, 4) for nuclear immunopositivity in the alveolar septae and the intensity of the nuclear immunopositivity of alveolar macrophages].

Expression profiling and pathway analysis

A whole human genome microarray 4 $\times$ 44k (Agilent #G4112F) was used to analyze the effects of LY2109761 on irradiated primary human fibroblasts (PromoCell). Cells were grown to a density of 70% in fibroblast growth medium 2 with 10% FCS (PromoCell), treated with 1 μmol/L LY2109761, 2 hours before 4 Gy radiation and harvested 6 hours after radiation for RNA isolation using miRNeasy Mini Kit (Qiagen #217004). The experiments were carried out at least in triplicate. Data were extracted with Agilent feature extraction software (Agilent version 9.1) and analyzed. We considered genes which were substantially ($\geq$2-fold) and significantly ($P < 0.05$) regulated. Ingenuity Pathway Analysis (IPA; www.ingenuity.com, Ingenuity Systems, Inc.) was used for analysis.

Protein analysis

Primary human fibroblasts were treated as described for expression profiling [additional treatment: 2 ng/mL TGF-β (TGF-β1), PromoCell # C-63505]. The experiments were carried out at least in triplicate. Protein was extracted 15, 30 minutes, 1, 2, 6, 24, and 48 hours after radiation with Qproteome (# 37900; Qiagen). Antibodies for Western blotting were: SMAD2 (Cell signaling; 3122) and phospho-SMAD2 (Cell signaling; 3108), SMAD1 (Cell signaling; 9743) and p-SMAD1 463/465 (Cell signaling; 9516), p38 (R&D), p-p38 (R&D; AF869), c-jun-NH$_2$-kinase (JNK, R&D; mab2076), p-JNK (R&D; af1205), and smooth muscle actin (SMA; Abcam ab5694-100).

Statistics

Data are expressed as means $\pm$ SDs. For comparisons between more than 2 groups ANOVA was used followed by the appropriate post hoc test or ANOVA for repeated measurements. All tests were 2-tailed. P less than 0.05 was considered statistically significant. Mouse survival curves were calculated with the Kaplan–Meier method and compared using the log-rank test using Statistica 6.0 software (Statsoft). The numbers of animals were derived from previous experiments using the same model (16–18) and pilot studies with the primary goal to reach statistical power to show differences in survival, in HU units in VCT, and in the number of inflammatory cells in histology between LY-treated and non-LY–treated irradiated groups.

Results

LY2109761 improves clinical status and survival after thoracic irradiation

We found that thoracic radiation with 20 Gy significantly reduced the life span of mice (Fig. 2A) with a median survival of only 120 days. In contrast, mice treated for 4 weeks with LY2109761 had a median survival of 160 days (all LY2109761 + RT-groups vs. RT-group, $P < 0.01$, log-rank). Mice with an early LY2109761 treatment start after radiation (RT, LY) showed the best survival ($P = 0.03$ vs. RT). When LY2109761 started before radiation [(LY, RT, LY), (LY, RT)] survival tended to improve, but without statistical significance ($P = 0.18$ and $P = 0.2$ vs. RT, respectively). Mice receiving LY2109761 only (LY) had similar long survival as sham-treated control animals. Together, these data show that 4-week treatment with LY2109761 improved survival after thoracic radiation.

Thoracic radiation also reduced mice body weights (Fig. 2B), which was partially attenuated by LY2109761 in all groups accompanied by improvements of other clinical parameters such as general animal behavior, tachypnea (higher after radiation, lower in combination with LY2109761), and heart rate (higher after radiation, lower in combination with LY2109761).

VCT of mice lungs

By 6 weeks after radiation, the VCT lung signal density significantly increased with several foci distributed over the
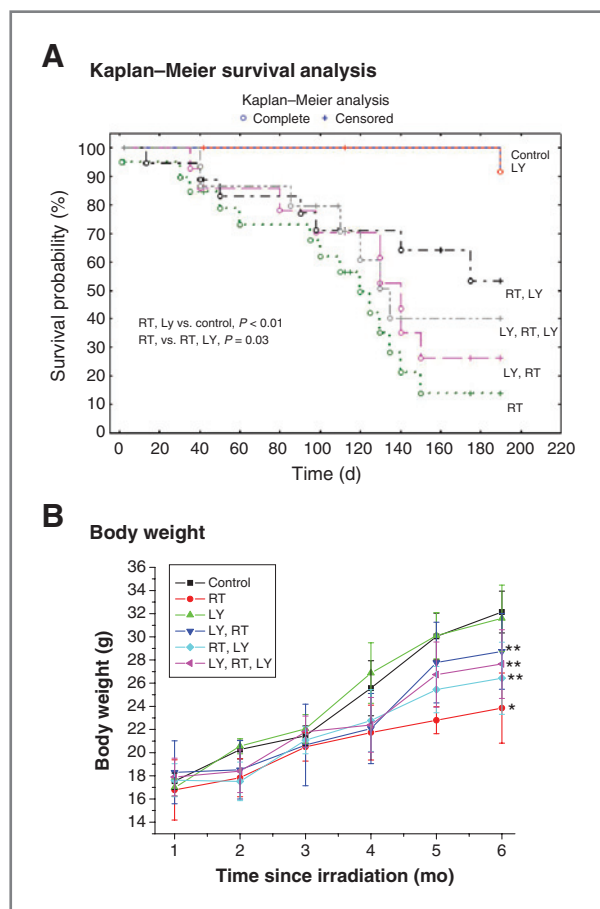
Figure 2. Clinical status and survival. A, Kaplan–Meier analysis of mouse survival after thoracic radiation and LY2109761 treatment. Radiation-reduced survival ($P < 0.01$ vs. control or LY2109761 alone, log-rank). LY2109761 alone had no influence on survival. LY2109761 treatment prolonged survival of irradiated mice (all LY + RT pooled vs. RT, $P < 0.01$). LY2109761 after the radiation (RT, LY vs. RT, $P = 0.03$) had the best effect on survival, whereas other schedules did not reach statistical significance (LY, RT vs. RT, $P = 0.2$; LY, RT, LY vs. RT, $P = 0.18$). The 3 mice sacrificed for histology were censored at the respective time points. B, body weights of mice were measured as a general measure of clinical status of mice. Irradiated mice (RT) had significantly reduced weight (*, $P < 0.03$ vs. controls and LY only). LY2109761-treated groups attenuated the radiation-associated weight loss (**, $P < 0.05$ vs. RT). Bars are mean ± SD.

entire lungs as typical signs of acute and subacute pneumonitis. Until week 20, the average lung densities further increased and the dense foci fused to larger areas, indicative of extensive lung fibrosis (Fig. 3A and B). The morphologic VCT images were consistent with reticular alterations and irregular septal thickening observed in histology (Fig. 4), which are typical CT findings of pulmonary fibrosis. In mice treated with LY2109761 these morphologic signs of subacute and chronic damage were drastically reduced. LY2109761 also markedly reduced the average lung densities in irradiated lungs. The magnitude of the reduction of average lung densities increased from 6 weeks to 20 weeks.

For example the group experiencing the largest benefit (RT, LY) showed a reduction of approximately 20 HU at 6 weeks, 100 HU units at 16 weeks, and 150 HU units at 20 weeks. Thus, the VCT data indicated that LY2109761 attenuated radiation-induced fibrosis but also reduced subacute lung injury.

MRI of mice lungs

MRI was used as an additional independent noninvasive radiological monitoring method to visualize morphologic changes, such as fibrotic remodeling of lung architecture, and functional changes, such as interstitial edema formation. Supporting the VCT findings, T1-weighted spin echo sequences showed areas of hyperintense signals as signs of increased lung density developing 6 weeks after radiation. The MRI examinations 16 and 20 weeks after radiation revealed a gradual progression leading to diffuse hyperintense signals over the entire lung (Fig. 3C). In few (2 of 12) animals the T2-weighted MRI sequence in addition showed areas of hyperintensity indicative of fluid accumulation. Therefore, the radiological interpretation together with the increased lung density seen by VCT was progressive fibrosis of the lung parenchyma, and in a few cases a mixture of fibrosis and alveolar or interstitial edema.

All LY2109761 treatment groups showed markedly reduced signs of pulmonary fibrosis in T1-weighted and Flash 3D sequences. Moreover, the T2-weighted imaging did not reveal signs of pulmonary edema or pleural effusion. Thus, LY2109761 attenuated both lung fibrosis, the potential lung edema formation after radiation, as well as earlier subacute lung injury.

Lung histology

Compared with nonirradiated mice, H&E, Goldner-Elastica, and Sirius Red staining showed concordantly that radiation induced severe acute, subacute, and chronic lung toxicity (Fig. 4A–D). Wall thickening and collagen deposition increased from day 2 to weeks 6, 16, and 20. The alveolar epithelium consists of type I and II epithelial cells in an almost balanced numeric proportion. Type I cells cover approximately 90% of the alveolar surface and type II pneumocytes represent the replicator precursors of type I cells. Pneumocyte type I damage was visible by week 6. Radiation-induced damage is thought to lead to the depletion of pneumocytes type I and proliferation of pneumocytes type II to restore epithelial continuity and production of surfactant, although radiation is toxic to type II pneumocytes as well (2, 6, 20). One possible mechanism is the induction of apoptosis primarily in pneumocytes type I (21).

We found consistent late changes related to radiation such as alterations in the epithelium of bronchi and bronchioles, including erosion, hyperplasia, and squamous metaplasia. The broadening of the alveolar septa along with collagen deposition at week 20 was suggestive of fibrosis. LY2109761 strongly attenuated the alterations including erosion, wall broadening, and collagen deposition, irrespective of the administration schedule (Fig. 4A–E).

Figure 3. Noninvasive radiological lung monitoring. A, representative VCT imaging of mouse lungs at week 20 after radiation to the thorax. Lung fibrosis is characterized by diffuse bilateral areas of "ground-glass" attenuation and intralobular reticular opacities (only RT). LY2109761 attenuates this radiological character (LY, RT; RT, LY; image for LY, RT, LY similar). Imaging of untreated control (no RT) and LY only is similar. B, quantitative lung density (modified Hounsfield) values derived from VCT scans at week 20 showing that LY2109761 reduces lung density which is enhanced after radiation. Three randomly chosen mice in each treatment arm were examined in a longitudinal study by VCT every 2 weeks. Eight ROIs were randomly selected in the lungs, and the lung density was determined for each ROI. Bars are mean $\pm$ SD. (*, $P < 0.05$ vs. only RT). C, representative MRIs (Flash 3D, SE-T1 and TSE-T2 sequences) of mouse lungs at week 20 after radiation. Normal MRI morphology in control- and LY2109761-treated animals (*). Characteristic diffuse hyperintense signals in Flash, T1-, and T2-weighed images (**, lung fibrosis) after radiation and one example of pulmonary edema (***) in T2 visible as vast hyperintensity. The MRI signs for RILI and RILF were reduced in LY2109761-treated groups. Imaging of untreated control (no RT) and LY only is similar, and imaging of LY, RT, LY is similar to LY, RT and RT, LY.
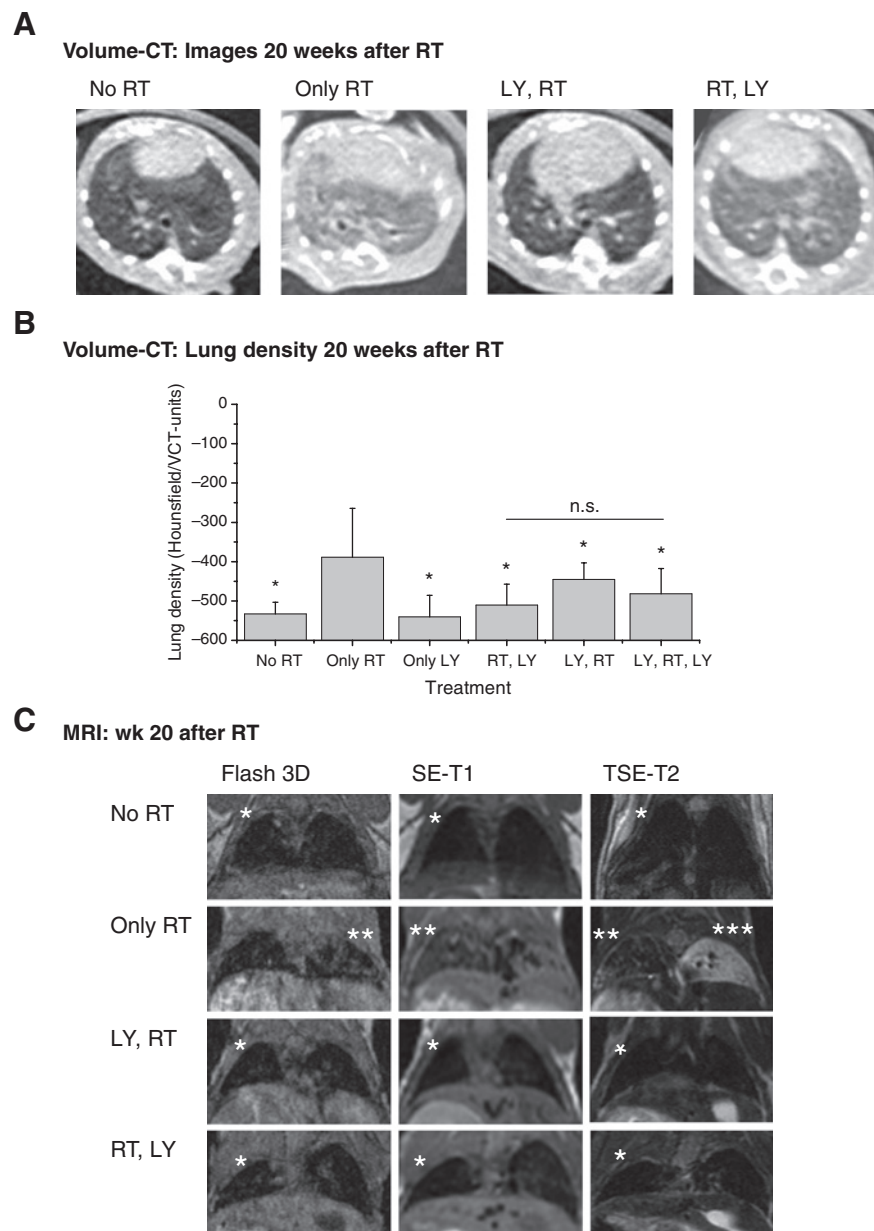
Intra-alveolar edema did not occur whereas some animals had formation of fibrillar or crystalline protein deposits within alveolar spaces.

LY2109761 also modulated radiation-induced infiltration of the lung tissue with inflammatory cells: two days after radiation predominantly leukocytes with some lymphocytes were present in the perivascular space and in alveolar septae, which subsided after 2 weeks (Fig. 4F). Interestingly, the second inflammation at weeks 16 to 20 with 4 times more leukocytes than in the acute inflammatory phase was associated with septal fibrosis development (Fig. 4G). Similarly, alveolar histiocytosis determined by the number of macrophages increased after week 16 in irradiated mice. LY2109761 strongly reduced the number of inflammatory cells in the acute phase around day 2 after radiation and during the later fibrogenesis-associated inflammation after week 16. Immunohistochemical assessment of canonical TGF-β signaling in the lungs showed that radiation increased SMAD2 phosphorylation in the nuclei of bronchial cells, the bronchiolar epithelium, and in macrophages (Fig. 4D and E). LY2109761 reduced the amount of p-SMAD2 in bronchiolar and alveolar
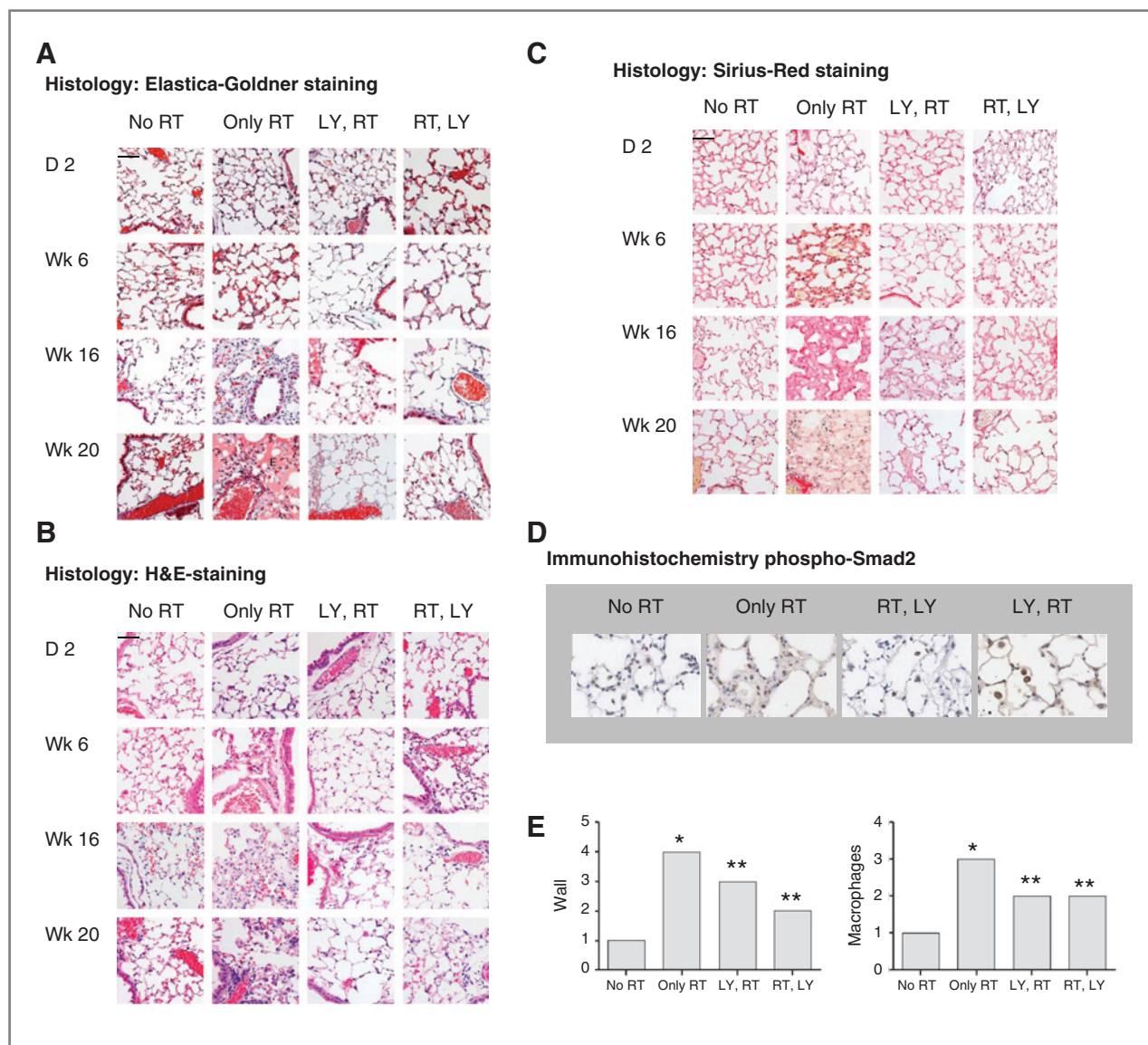
Figure 4. Lung histology. Representative examples of histology of mouse lungs treated with 20 Gy ± LY2109761 at day 2, weeks 6, 16, 20 after the irradiation. Radiation-induced increasing wall thickening and collagen deposition along with alterations in the epithelium of bronchi and bronchioles, and in some cases edema; all were attenuated by LY2109761. Untreated control (no RT) and LY only is similar and LY, RT, LY is similar to LY, RT and RT, LY. A, Goldner–Elastica. B, H&E. C, Sirius Red. D, representative examples of immunohistochemistry of lung tissue at week 20 after radiation. Phospho-smad2 nuclear immunopositivity is displayed. E, the amount of nuclear immunopositivity in the alveolar septae and the intensity of the nuclear immunopositivity of alveolar macrophages were scored on a rank scale base (0, 1, 2, 3, 4). Bars are median (*, $P < 0.05$ vs. radiation, RT).

epithelium and reduced the intensity of the nuclear immunopositivity of alveolar macrophages.

LY2109761 reverses radiation-induced proangiogenic and proinflammatory signaling

Transcriptomic evaluation in fibroblasts showed that radiation alone regulated 190 genes, LY2109761 491 genes, and the combination LY2109761 + radiation regulated 484 genes by more than 2-fold (Fig. 5). Biologic function assignment using "gene ontology" terms (GO terms, Supplementary Table S1) showed that within the GO term "TGF-β/BMP signaling," radiation increased TGF-β1 expression which was decreased by LY2109761. Likewise, radiation increased Gremlin (Grem2), ID1, Smad 6, 7, and 9 expressions, whereas LY2109761 markedly decreased their expression even in the presence of radiation. Moreover, LY2109761 also decreased expression of Fos, KLF10, MDM2, GDF15, and FAS, alone and in combination with radiation. Furthermore, LY2109761 reduced the expression of mitogen-activated protein kinase (MAPK)3 and 13 which are also associated with fibrosis development.

Figure 4. (*Continued*) F, inflammatory cells. Leukocytes in mouse lung tissue as a correlate of inflammation at 2 days and 20 weeks after the thoracic radiation. Bars are mean ± SD [*, $P < 0.05$ vs. radiation (only RT)]. G, septal thickness in mouse lung tissue at 2 days and 20 weeks after the thoracic radiation quantified as described in Methods. Bars are mean ± SD [*, $P < 0.05$ vs. radiation (only RT)]
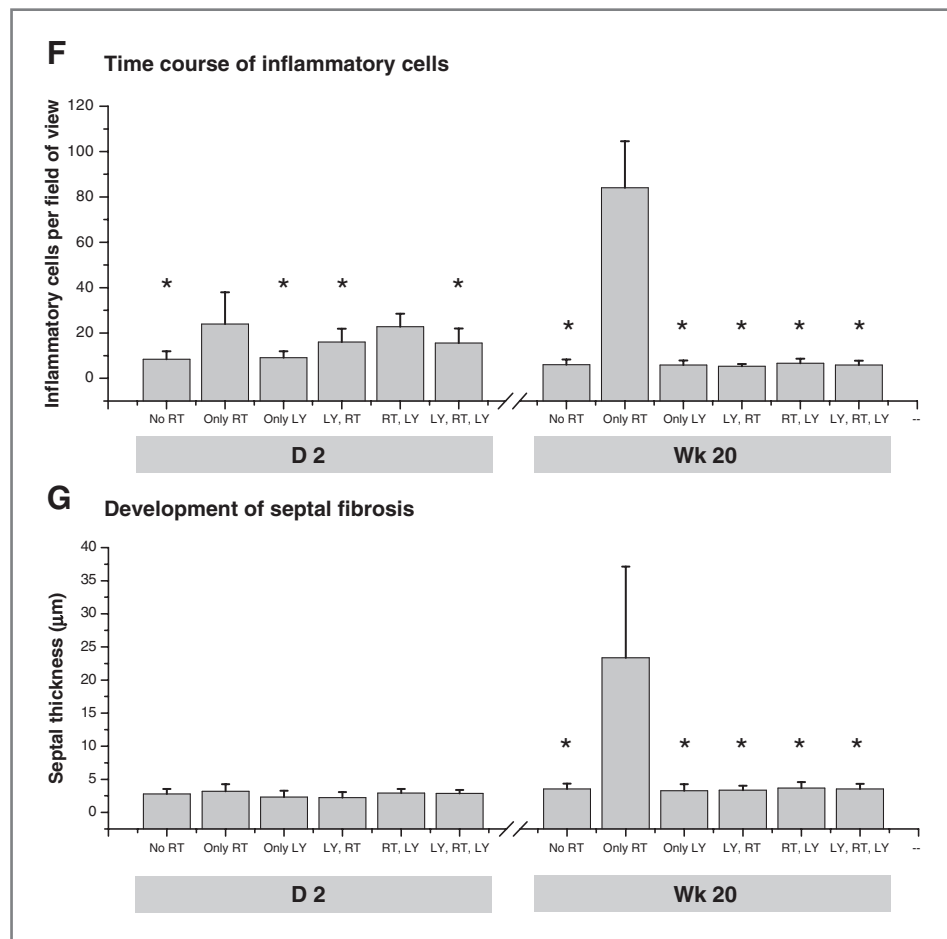
In contrast, LY2109761 induced BMP2 and members of the TNF receptor superfamily 11B, 19, and tissue factor F3, which were hardly affected by radiation.

Importantly, LY2109761 also downregulated other genes involved in inflammation signaling including IL-6, IL-7R, and IL-8, whereas some of these genes were upregulated after radiation (Table 1). Interestingly, with respect to angiogenesis as an important part of wound healing and thus fibrosis formation, LY2109761 also reduced the expression of proangiogenic genes such as ID1, ID2, and ID3 compared with radiation treatment. Together, expression analysis showed that LY2109761 attenuated downstream signals from TGF-β and BMP and reversed proinflammatory and proangiogenic signals which were partially upregulated by radiation (Fig. 5C).

Protein analysis

Protein analysis showed that TGF-β1 treatment strongly induced phosphorylation of SMAD2 after 15 minutes lasting up to 48 hours without marked effects on SMAD2 levels in fibroblasts (Fig. 5D). Neither radiation nor LY2109761 had marked effects on SMAD2 or p-SMAD2 expression. Interestingly, phosphorylation of Smad1 was slightly enhanced up to 2 hours after radiation, which was markedly attenuated by LY2109761. Smad1 was hardly affected by either radiation or LY2109761. Two proteins involved in noncanonical TGF-β signaling, p38 and JNK, were also phosphorylated after radiation and showed a further phosphorylation increase after the addition of LY2109761 up to 6 hours. SMA protein levels as a myofibroblast and pericyte marker involved in vessel stabilization exhibited a moderate but constant increase from 15 minutes to 48 hours after radiation which was slightly reduced by LY2109761.

Discussion

Our study indicates that oral administration of the small-molecule TGF-βR inhibitor LY2109761 for 4 weeks could significantly reduce the formation of acute and subacute RILI and RILF in C57Bl/6 mice. Furthermore, our findings suggest that mouse survival, which is markedly reduced after radiation, can be prolonged by LY2109761. These beneficial effects were especially present if the TGF-β blockade started after radiation. Likewise, the compromised general clinical status after radiation such as tachypnea and increased heart rate was improved by LY2109761. In summary, these data suggest that small-molecule TGF-βR kinase inhibitors may serve as a relevant supplemental therapy or alternative to corticosteroids for RILI treatment.
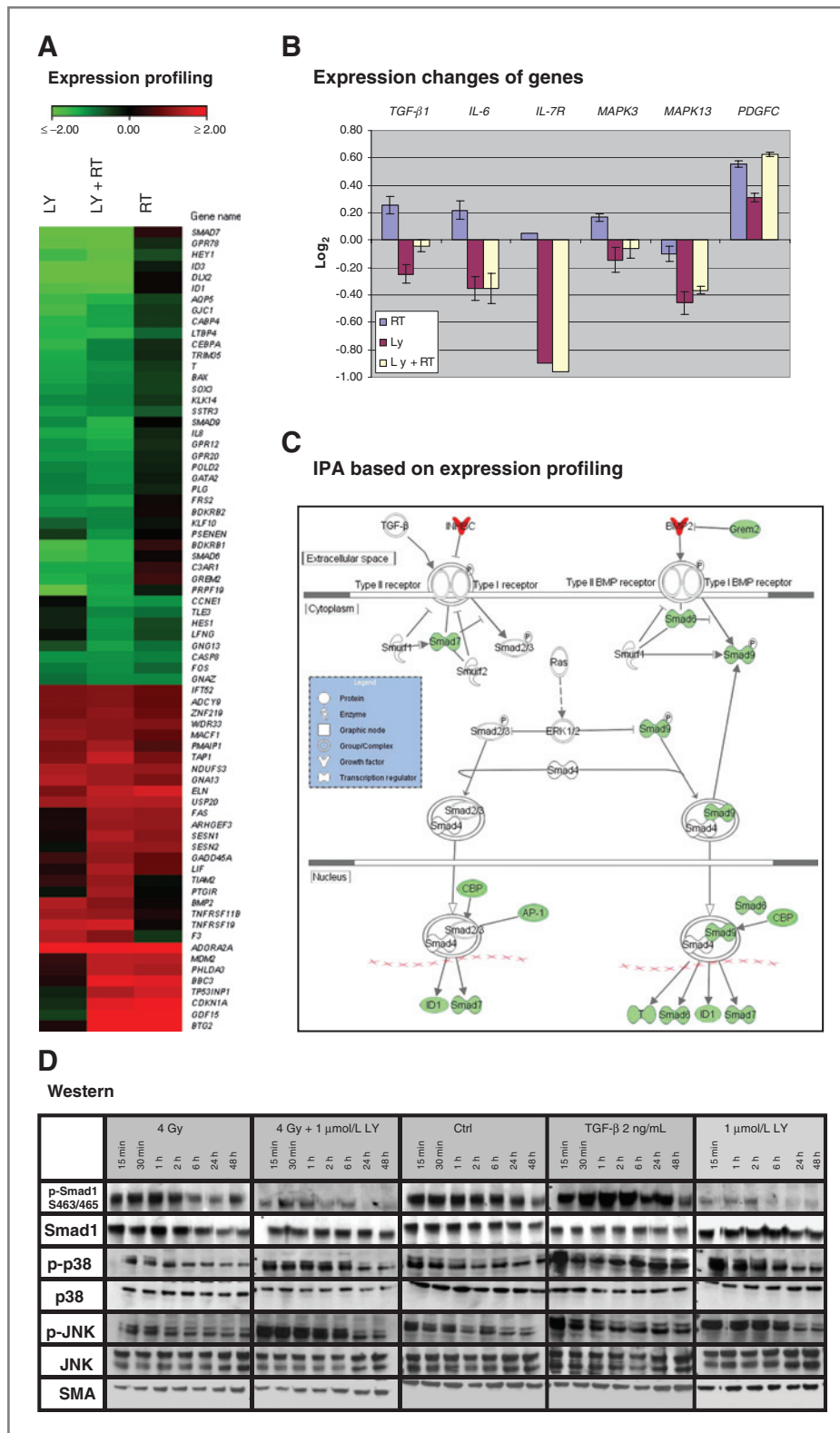
Figure 5. Signaling analysis. A, gene expression measured with genome-wide DNA array with RNA extracted from human primary fibroblasts 6 hours after treatments. Heatmap of more than 2-fold–regulated genes after treatment with 1 μmol/L LY2109761 + 4 Gy (LY + RT) from GO: 0007165 "signal transduction." The gene regulation is presented as the ratio of treatment/control value. Color scale from log₂ value −2 (bright green) to 2 (bright red). B, expression changes of genes involved in inflammation and/or TGF-β signaling after treatment of primary fibroblasts. Bars are mean log2 value of regulation (treatment/control) ± SD. C, IPA of regulated genes in TGF-β and BMP signaling. Genes more than 2-fold regulated after treatment with LY2109761 and RT are colored in red (activated) or green (inhibited). D, Western blot analysis of protein extracts from primary fibroblasts treated with radiation (4Gy, RT), LY2109761, and TGF-β.

After radiation, we monitored the mice lungs by noninvasive radiological methods allowing for morphologic and quantitative longitudinal studies over the entire observation period of more than 6 months. The novel computed tomography method for animal imaging, VCT, and MRI scans concordantly revealed significantly increased lung density values in irradiated mice as radiological correlates for pulmonary fibrosis. In the areas of condensed lung

Table 1. Fold mRNA regulation of selected genes after LY treatment in human fibroblasts

Gene name	Fold regulation by LY
ID1	0.28
ID2	0.29
IL-6	0.78
IL-7R	0.54
IL-8	0.41
BMP2	2.62
TGF-β1	0.84
Grem2	0.39
TNFRSF11B	2.05
TNFRSF19	2.93
TFF1	3.19
SMAD6	0.33
SMAD7	0.18
SMAD9	0.48
Fos	0.52
KLF10	0.6
MDM2	1.39
GDF15	0.7

parenchyma, reticular alterations and septal thickening were present as morphologic signs of progressive fibrotic reformation of lung tissue. Importantly, the radiological signs and density values were markedly reduced in mice treated with LY2109761. In accordance with the radiological findings, the histologic assessment showed that LY2109761 reduced the pathologic infiltration with inflammatory cells, the formation of fibroblast foci, and the deposition of extracellular matrix leading to septal thickening with subsequent impaired lung function.

The measurable antifibrotic effects determined by radiological and histologic means were present and similar irrespective of the LY2109761 administration start before, during, or after the radiation. However, the clinical and life span benefits as an integral measure of several, including unknown factors tended to be pronounced if LY2109761 started after the radiation. This suggests that LY2109761 targets especially processes related to later phases of radiation induced toxicity, although one cannot exclude partially negative combinatorial effects if the drug is given concurrently with radiation. One reason why the available data do not give us a definitive answer is that there was no LY group starting shortly before radiation whose administration interval would mostly overlap with the group (RT, LY) with an early treatment start after radiation. With respect to interactions of TGF-β inhibition and radiation, Kirshner and colleagues (22) had found in human mammary epithelial cells that a TGF-β-R1 inhibitor reduced the induction of radiation-induced γH2AX foci, but otherwise increased radiosensitivity. This result had prompted these authors to suggest that TGF-β inhibition in combination with radiotherapy might be a strategy as cancer therapeutic. While we

agree for the cancer case as shown in a report in glioblastoma (23), the report by Kirshner and colleagues may also suggest that there are toxic effects in normal cells if radiation and TGF-β inhibition is given simultaneously. Such effects may be present in lung epithelium/endothelium and might be one reason why giving the drug after the radiation event is beneficial to induce the beneficial effects of TGF-β inhibition on normal cells. Aside from this issue, it is possible that the TGF-β signaling relevant events or the fibrogenesis relevant events occur later after radiation, which may suggest that a later intervention is simply preferable with respect to a better antifibrotic effect.

Immunohistochemistry and expression profiling further revealed effects of LY2109761 on TGF-β signaling, inflammation, and angiogenesis. Like other cytokines, including platelet-derived growth factor (PDGF), TNF-α, and IL-1, TGF-β is upregulated by radiation (24). An involvement of TGF-β in fibrogenesis has been shown for several tissues, and TGF-β induced by radiation has been reported as part of radiation-induced fibrosis (1–3, 6, 12).

Accordingly, our gene expression analysis showed radiation-induced activation of genes involved in DNA damage response, cell-cycle arrest, induction of apoptosis, inflammation, and angiogenesis. While gene expression associated with DNA damage response, cell-cycle arrest, induction of apoptosis were almost unchanged, LY2109761 induced marked changes in BMP and TGF-β signaling cascades, which were hardly affected by radiation.

Moreover, LY2109761 reduced the expression of genes associated with inflammation like IL-6, IL-8, IL-7R, and Fos, whereas radiation increased their expression. This is consistent with other inflammation models showing increased IL-6, IL-8, and TGF-β levels (25, 26).

Because scar formation and formation of fibrosis are dependent on blood supply and neoangiogenesis, inhibition of angiogenesis might add to the antifibrotic effects of LY2109761 in vivo. Accordingly, we found that LY2109761 strongly reduced the expression of proangiogenic genes such as ID1, ID2, and ID3.

A balanced TGF-β and BMP signaling is important for stereoblastic differentiation. BMP7 antagonizes TGF-β–dependent renal fibrogenesis (13), and TGF-β/activin but neither BMP7 nor BMP type I can induce epithelial–mesenchymal transition (EMT; ref. 27). Furthermore, the BMP2, -4, and -7 antagonist Gremlin is highly upregulated in human IPF and asbestos-induced mouse fibrosis (28). Our data suggest that LY2109761 attenuates profibrotic signaling directly, but also balances the complex TGF-β/BMP signaling: LY2109761 dramatically reduced radiation-induced upregulation of Gremlin (Grem2) and also upregulated BMP2 expression. Moreover, LY2109761 reduced radiation-induced downstream signaling genes of TGF-β including Smads 6, 7, and 9 but also MDM2 in accordance with lung histology showing reduced p-Smad2, with increased p-Smad2 levels being associated with lung fibrosis (29). While radiation slightly increased and LY2109761 clearly decreased Smad1 phosphorylation, Smad2 or Smad3 phosphorylation was hardly affected in

fibroblasts. Despite elevated TGF-β1 transcription upon irradiation activation of TGF-β protein was apparently insufficient to induce the canonical Smad2/Smad3 pathway in this setting.

Interestingly, LY2109761 strongly decreased Smad1 phosphorylation despite a strong increase of BMP2 transcripts. Smad1 is an important part of the noncanonical TGF-β pathway and phosphorylation target of ALK1/2/3 and 6 receptors specifically activated by BMPs (15, 30). Therefore, our data suggest that LY2109761 is also a potent inhibitor of BMP receptor signaling. This notion is strengthened by the finding, that ID1 expression, which can be induced by BMP via Smad1 phosphorylation (31), was repressed by LY2109761. We also detected increased phosphorylation of JNK and p38 after LY2109761 treatment. BMP2 and TGF-β had been shown to induce p38 and JNK phosphorylation independent of Smad pathways, although downstream cellular responses can be mediated by interactions with Smad pathways (32, 33). The observation that downstream of the SMAD inhibition other kinases may be altered in the phosphorylation profile has been also reported for LY2109761 in HCC lines, primarily for the AKT/mTOR pathway (34). Furthermore, it is possible that the increased BMP2 mRNA expression and JNK/p38 phosphorylation after LY2109761 treatment represent an escape mechanism once the TGF-β receptor signaling is inactivated. This result further supports the understanding of the beneficial effects of LY2109761 on radiation toxicity, because the downregulated MAPKs downstream from BMPs have been proposed as therapeutical targets in chronic obstructive pulmonary disease (35). Together, these data may suggest that LY2109761 has also antifibrotic effects via inhibition of BMP signaling.

Alternatively or in addition, pulmonary stem cells (36) may be involved in fibrogenesis. Because TGF-β1 signaling has been associated with differentiation of stem cells in other disease models such as GBM (37), the stem cell hypothesis may be of relevance in our fibrosis model.

It is conceivable that the reduction of pulmonary fibrosis by LY2109761 is due to a combination of several mechanisms: one mechanism is the direct inhibition of Smad-dependent and Smad-independent pathways in the TGF-β and BMP family signaling. Other explanations for the antifibrotic effects of LY2109761 include indirect effects on the microenvironment such as anti-inflammatory and antiangiogenic effects. These latter findings are also in agreement with a recent report on the antiangiogenic effects of LY2109761 via ID1 suppression in a glioblastoma model in mice (37). Moreover, our results are in agreement with our own recent data showing that LY2109761 may be effective as anticancer compound via potentiation of radiation response in glioblastoma by coordinately targeting cancer stem–like cells while blocking DNA damage repair, invasion, mesenchymal transition, and tumor angiogenesis (38). Interestingly, together these data suggest that the same compound is effective as anticancer therapeutic and as anti-inflamma-

tion/antifibrosis therapeutic which links fibrosis and cancer. Noteworthy, the signaling events apparently associated with the respective beneficial therapeutic events appear to be strikingly similar thus linking fibrosis and cancer therapy.

Physiologic processes are in general balanced and finely tuned by positive and negative regulatory mechanisms (39). A prototypical process is the angiogenic switch in tumors which is regulated by a multitude of signaling circuitries (40). Fibrosis as result of an exaggerated wound-healing reaction may similarly reflect an imbalance of a homeostatic system composed of such elements (41–43). LY2109761 appears to shift the genetic balance using several circuitries resulting in an antifibrotic phenotype with reduced RILI and RILF.

Inhibitors of PDGF, VEGF, and fibroblast growth factor (FGF) have been shown to attenuate lung fibrosis in bleomycin models (44, 45), and TGF-β antibodies as well as a different small-molecule TGF-β kinase inhibitor were studied in a radiation-induced lung prevention fibrosis model in rats (46–48). Similarly, simvastatin has recently been shown to attenuate acute RILI without affecting later fibrosis or mouse survival (48). Our report here shows for the first time beneficial effects of a TGF-β kinase inhibitor on survival in a mouse model of fibrosis along with quantitative VCT and MRI *in vivo* lung monitoring.

In summary, the inhibition of TGF-β signaling seems a promising strategy to attenuate RILI and RILF. An interesting finding was that the overall radioprotection was actually better if the drug was given after radiation exposure. This has potentially important implications in the clinic, as well as in the setting of accidental or terrorist-related exposures. One clinical relevance arises from the large number of patients undergoing radiotherapy of non–small cell lung cancer (NSCLC; ref. 49). In such patients an oral therapeutic poses an attractive combination treatment option. Next experimental steps to bring the principle of TGF-β inhibition into the clinic may include investigations on optimizing the time interval between drug treatment and irradiation as well as the conduction of phase I trials in patients who are candidates for single high-dose radiotherapy for therapy of lung tumors. It might also be interesting to investigate if fibrosis in other organs or of different origin can be attenuated by such drugs.

Disclosure of Potential Conflicts of Interest

Acknowledgments

Grant Support

References

1. Rubin P, Johnston CJ, Williams JP, McDonald S, Finkelstein JN. A perpetual cascade of cytokines postirradiation leads to pulmonary fibrosis. Int J Radiat Oncol Biol Phys 1995;33:99–109.

2. Vujaskovic Z, Marks LB, Anscher MS. The physical parameters and molecular events associated with radiation-induced lung toxicity. Semin Radiat Oncol 2000;10:296–307.

3. Travis EL. Early indicators of radiation injury in the lung: are they useful predictors for late changes? Int J Radiat Oncol Biol Phys 1980;6:1267–9.

4. Kwok E, Chan CK. Corticosteroids and azathioprine do not prevent radiation-induced lung injury. Can Respir J 1998;5:211–4.

5. Delanian S, Lefaix JL. Current management for late normal tissue injury: radiation-induced fibrosis and necrosis. Semin Radiat Oncol 2007;17:99–107.

6. Tsoutsou PG, Gourgoulianis KI, Petinaki E, Mpaka M, Efremidou S, Maniatis A, et al. ICAM-1, ICAM-2 and ICAM-3 in the sera of patients with idiopathic pulmonary fibrosis. Inflammation 2004;28:359–64.

7. Mason RJ, Schwarz MI, Hunninghake GW, Musson RA. NHLBI Workshop Summary. Pharmacological therapy for idiopathic pulmonary fibrosis. Past, present, and future. Am J Respir Crit Care Med 1999;160:1771–7.

8. Gross TJ, Hunninghake GW. Idiopathic pulmonary fibrosis. N Engl J Med 2001;345:517–25.

9. Massague J, Like B. Cellular receptors for type beta transforming growth factor. Ligand binding and affinity labeling in human and rodent cell lines. J Biol Chem 1985;260:2636–45.

10. Broekelmann TJ, Limper AH, Colby TV, McDonald JA. Transforming growth factor beta 1 is present at sites of extracellular matrix gene expression in human pulmonary fibrosis. Proc Natl Acad Sci U S A 1991;88:6642–6.

11. Border WA, Noble NA. Transforming growth factor beta in tissue fibrosis. N Engl J Med 1994;331:1286–92.

12. Rube CE, Uthe D, Schmid KW, Richter KD, Wessel J, Schuck A, et al. Dose-dependent induction of transforming growth factor beta (TGF-beta) in the lung tissue of fibrosis-prone mice after thoracic irradiation. Int J Radiat Oncol Biol Phys 2000;47:1033–42.

13. Yingling JM, Blanchard KL, Sawyer JS. Development of TGF-beta signalling inhibitors for cancer therapy. Nat Rev Drug Discov 2004;3:1011–22.

14. Nishioka A, Ogawa Y, Mima T, Jin YJ, Sonobe H, Kariya S, et al. Histopathologic amelioration of fibroproliferative change in rat irradiated lung using soluble transforming growth factor-beta (TGF-beta) receptor mediated by adenoviral vector. Int J Radiat Oncol Biol Phys 2004;58:1235–41.

15. Derynck R, Zhang YE. Smad-dependent and Smad-independent pathways in TGF-beta family signalling. Nature 2003;425:577–84.

16. Abdollahi A, Li M, Ping G, Plathow C, Domhan S, Kiessling F, et al. Inhibition of platelet-derived growth factor signaling attenuates pulmonary fibrosis. J Exp Med 2005;201:925–35.

17. Flechsig P, Hartenstein B, Teurich S, Dadrich M, Hauser K, Abdollahi A, et al. Loss of matrix metalloproteinase-13 attenuates murine radiation-induced pulmonary fibrosis. Int J Radiat Oncol Biol Phys 2010;77:582–90.

18. Plathow C, Li M, Gong P, Zieher H, Kiessling F, Peschke P, et al. Computed tomography monitoring of radiation-induced lung fibrosis in mice. Invest Radiol 2004;39:600–9.

19. Kiessling F, Greschus S, Lichy MP, Bock M, Fink C, Vosseler S, et al. Volumetric computed tomography (VCT): a new technology for non-invasive, high-resolution monitoring of tumor angiogenesis. Nat Med 2004;10:1133–8.

20. Trott KR, Herrmann T, Kasper M. Target cells in radiation pneumopathy. Int J Radiat Oncol Biol Phys 2004;58:463–9.

21. Zhang Y, Zhang X, Rabbani ZN, Jackson IL, Vujaskovic Z. Oxidative stress mediates radiation lung injury by inducing apoptosis. Int J Radiat Oncol Biol Phys. 2012 Jan 21. [Epub ahead of print].

22. Kirshner J, Jobling MF, Pajares MJ, Ravani SA, Glick AB, Lavin MJ, et al. Inhibition of transforming growth factor-beta1 signaling attenuates ataxia telangiectasia mutated activity in response to genotoxic stress. Cancer Res 2006;66:10861–9.

23. Zhang M, Herion TW, Timke C, Han N, Hauser K, Weber KJ, et al. Trimodal glioblastoma treatment consisting of concurrent radiotherapy, temozolomide, and the novel TGF-beta receptor I kinase inhibitor LY2109761. Neoplasia 2011;13:537–49.

24. Johnston CJ, Piedboeuf B, Rubin P, Williams JP, Baggs R, Finkelstein JN. Early and persistent alterations in the expression of interleukin-1 alpha, interleukin-1 beta and tumor necrosis factor alpha mRNA levels in fibrosis-resistant and sensitive mice after thoracic irradiation. Radiat Res 1996;145:762–7.

25. Reibman J, Meixler S, Lee TC, Gold LI, Cronstein BN, Haines KA, et al. Transforming growth factor beta 1, a potent chemoattractant for human neutrophils, bypasses classic signal-transduction pathways. Proc Natl Acad Sci U S A 1991;88:6805–9.

26. Goulet S, Bihl MP, Gambazzi F, Tamm M, Roth M. Opposite effect of corticosteroids and long-acting beta(2)-agonists on serum- and TGF-beta(1)-induced extracellular matrix deposition by primary human lung fibroblasts. J Cell Physiol 2007;210:167–76.

27. Valcourt U, Kowanetz M, Niimi H, Heldin CH, Moustakas A. TGF-beta and the Smad signaling pathway support transcriptomic reprogramming during epithelial-mesenchymal cell transition. Mol Biol Cell 2005;16:1987–2002.

28. Myllarniemi M, Lindholm P, Ryynanen MJ, Kliment CR, Salmenkivi K, Keski-Oja J, et al. Gremlin-mediated decrease in bone morphogenetic protein signaling promotes pulmonary fibrosis. Am J Respir Crit Care Med 2008;177:321–9.

29. Higashiyama H, Yoshimoto D, Okamoto Y, Kikkawa H, Asano S, Kinoshita M. Receptor-activated Smad localisation in bleomycin-induced pulmonary fibrosis. J Clin Pathol 2007;60:283–9.

30. Sapkota G, Alarcon C, Spagnoli FM, Brivanlou AH, Massague J. Balancing BMP signaling through integrated inputs into the Smad1 linker. Mol Cell 2007;25:441–54.

31. Zhang YE. Non-Smad pathways in TGF-beta signaling. Cell Res 2009;19:128–39.

32. Jun D, Garat C, West J, Thorn N, Chow K, Cleaver T, et al. The pathology of bleomycin-induced fibrosis is associated with loss of resident lung mesenchymal stem cells that regulate effector T-cell proliferation. Stem Cells 2011;29:725–35.

33. Nohe A, Keating E, Knaus P, Petersen NO. Signal transduction of bone morphogenetic protein receptors. Cell Signal 2004;16:291–9.

34. Fransvea E, Mazzocca A, Santamato A, Azzariti A, Antonaci S, Giannelli G. Kinase activation profile associated with TGF-beta-dependent migration of HCC cells: a preclinical study. Cancer Chemother Pharmacol 2011;68:79–86.

35. Mercer BA, D'Armiento JM. Emerging role of MAP kinase pathways as therapeutic targets in COPD. Int J Chron Obstruct Pulmon Dis 2006;1:137–50.

36. Kajstura J, Rota M, Hall SR, Hosoda T, D'Amario D, Sanada F, et al. Evidence for human lung stem cells. N Engl J Med 2011;364:1795–806.

37. Anido J, Saez-Borderias A, Gonzalez-Junca A, Rodon L, Folch G, Carmona MA, et al. TGF-beta receptor inhibitors target the CD44(high)/Id1(high) glioma-initiating cell population in human glioblastoma. Cancer Cell 2010;18:655–68.

38. Zhang M, Kleber S, Roehrich M, Timke C, Han N, Tuettenberg J, et al. Blockade of TGF-beta signaling by the TGFbetaR-I kinase Inhibitor

LY2109761 enhances radiation response and prolongs survival in glioblastoma. Cancer Res 2011;71:7155–67

39. Wagner GP, Pavlicev M, Cheverud JM. The road to modularity. Nat Rev Genet 2007;8:921–31.

40. Abdollahi A, Schwager C, Kleeff J, Esposito I, Domhan S, Peschke P, et al. Transcriptional network governing the angiogenic switch in human pancreatic cancer. Proc Natl Acad Sci U S A 2007;104:12890–5.

41. Studer SM, Kaminski N. Towards systems biology of human pulmonary fibrosis. Proc Am Thorac Soc 2007;4:85–91.

42. Hauser K, Abdollahi A, Huber PE. Inverse system perturbations as a new methodology for identifying transcriptomic signaling participants in balanced biological processes. Cell Cycle 2009;8:2718–22.

43. Manfredi JJ. The Mdm2-p53 relationship evolves: Mdm2 swings both ways as an oncogene and a tumor suppressor. Genes Dev 2010;24: 1580–9.

44. Chaudhary NI, Roth GJ, Hilberg F, Muller-Quernheim J, Prasse A, Zissel G, et al. Inhibition of PDGF, VEGF and FGF signalling attenuates fibrosis. Eur Respir J 2007;29:976–85.

45. Anscher MS, Thrasher B, Rabbani Z, Teicher B, Vujaskovic Z. Anti-transforming growth factor-beta antibody 1D11 ameliorates normal tissue damage caused by high-dose radiation. Int J Radiat Oncol Biol Phys 2006;65:876–81.

46. Anscher MS, Thrasher B, Zgonjanin L, Rabbani ZN, Corbley MJ, Fu K, et al. Small molecular inhibitor of transforming growth factor-beta protects against development of radiation-induced lung injury. Int J Radiat Oncol Biol Phys 2008;71:829–37.

47. Anscher MS. Targeting the TGF-beta1 pathway to prevent normal tissue injury after cancer therapy. Oncologist 2010;15: 350–9.

48. Mathew B, Huang Y, Jacobson JR, Berdyshev E, Gerhold LM, Wang T, et al. Simvastatin attenuates radiation-induced murine lung injury and dysregulated lung gene expression. Am J Respir Cell Mol Biol 2010; 44:415–22.

49. Hof H, Mu enter M, Oetzel D, Hoess A, Debus J, Herfarth K. Stereotactic single-dose radiotherapy (radiosurgery) of early stage nonsmall-cell lung cancer (NSCLC). Cancer 2007;110:148–55.

Clinical Cancer Research

LY2109761 Attenuates Radiation-Induced Pulmonary Murine Fibrosis via Reversal of TGF- β and BMP-Associated Proinflammatory and Proangiogenic Signals

Paul Flechsig, Monika Dadrich, Sebastian Bickelhaupt, et al.

Updated version	Access the most recent version of this article at: doi:10.1158/1078-0432.CCR-11-2855
Supplementary Material	Access the most recent supplemental material at: http://clincancerres.aacrjournals.org/content/suppl/2012/04/30/1078-0432.CCR-11-2855.DC1

E-mail alerts	Sign up to receive free email-alerts related to this article or journal.
Reprints and Subscriptions	To order reprints of this article or to subscribe to the journal, contact the AACR Publications Department at pubs@aacr.org.
Permissions	To request permission to re-use all or part of this article, contact the AACR Publications Department at permissions@aacr.org.